



## Computational based approach in discovering the phytocompound based complex inhibition against *Ralstonia solanacearum* and root-knot nematode *Meloidogyne incognita*

Navyashree B<sup>1</sup>, Anisha S Jain<sup>1</sup>, Sushma P<sup>1</sup>, Chandan D<sup>1</sup>, Sharagouda S Patil<sup>2</sup>, Shiva Prasad Kollur<sup>3</sup>, Latha KC<sup>1,4</sup> and Chandan S<sup>1,\*</sup>

<sup>1</sup>Department of Biotechnology and Bioinformatics, Faculty of Life Sciences, JSS Academy of Higher Education and Research, Mysore-570011, Karnataka, India.

<sup>2</sup>ICAR-National Institute of Veterinary Epidemiology and Disease Informatics, Yelahanka, Bengaluru, India.

<sup>3</sup>Department of Sciences, Amrita School of Arts and Sciences, Amrita VishwaVidyapeetham, Mysuru campus – 570 026, Karnataka (India).

<sup>4</sup>University Grant Commission- South Western Regional Office (Bangalore), Bangalore, Karnataka-56009, India.

Email: [chandans@jssunil.edu.in](mailto:chandans@jssunil.edu.in)

### ABSTRACT

India is considered as a global agriculture powerhouse since ages, agriculture being the largest private enterprise in India, contributes a major part for the development and fulfillment of basic needs of Indian economy. Most of the Indian population say about 65% depend on agriculture as their traditional occupation. Infections to solanaceae plants has a worldwide economic importance since the disease is devastating to a large number of important crops and causes great losses in tomato. The bacterial wilt and the root knot nematodes are very tiny in nature and nematode make place on the plant and become the parasites, they give entry into the tomato root through small injuries and the eelworms are very common nematode found in the tomato root. Silver nanoparticles has shown evidence of being a potentially effective nematicide and its toxicity is associated with induction of oxidative stress in the cells of targeted nematodes. Usage of plant-derived antimicrobial agents might be effective in reducing the dependence on antibiotics and minimizing the chances of antibiotic resistance in food borne pathogenic microorganisms. In the present study, the author has made an attempt to evaluate the antimicrobial activities of phytocompounds of *Alstonia macrophylla* complexed with silver nanoparticles against *Ralstonia solanacearum* and root-knot nematode *Meloidogyne incognita*.

**Key words:** Solanaceae, nematode, nanoparticles, antimicrobial, *Ralstonia solanacearum*

Received 21.04.2021

Revised 06.07.2021

Accepted 09.09.2021

### INTRODUCTION

Tomato is the second most important vegetable crop next to potato. Present world production of tomato is about 100 million tons produced on 3.7 million hectares. The area harvested under tomato in India is 479200 ha, yield being 179169 hg/ha (hg = hectogram) and the production quantity is 8585800 tones [1]. The crop land varies from region to region, based on their soil type, nutritional status, weather, management practices etc. Argo-climatic condition also play an important role for the development of crops, were weather plays an important role. With the manufacturing sector agriculture derives its importance for vital supply and demand links. In past five years agriculture sectors shows a remarkable advance for production and productivity of vegetables, dairy, poultry, fruits, oilseeds, food grains etc. India stands second place for large producer of fruits and vegetables across the globe. Among various crops tomato is the most common staple food and stands second most important botanical fruit but a culinary vegetable [2].

20.6%. Root-knot nematodes (RKNs, *Meloidogyne* species) have broad host plant specificity and are responsible for > US\$125 billion annually in world-wide crop losses. Crops [3]. The most damaging of all root-knot nematodes is the southern RKN, *M. incognita*, which infects almost all agricultural plants including tomato. Biosynthetic of metal (Ag, Au, Cu and Cd) nano-formulation of plant extracts has received an increasing attention because of their potential application in pest control. AgNP has shown evidence of being a potentially effective nematicide [4] and its toxicity. Although most researchers have

investigated the antifungal, antiviral, and antibacterial activities of AgNPs, little attention has been given to nematocidal activities of such material. Therefore, the aim of this study was to evaluate the effectiveness of biological and chemical Ag-nano formulations against the root-knot nematode, *M. incognita*. Hence in the present study, an attempt has been made with the antimicrobial activity of extracts of certain selected medicinal plants on some human pathogenic bacteria [5]. In this study, methanol and petroleum ether extracts of two plants, which had been described in herbal books and folklore medicine of India, were screened for their antimicrobial activity.

There are many chemical controlling measures or fumigants available to prevent the nematodes. To prevent the toxic effect of the nematicide, the green synthesis method was adapted in the current study [6]. The leaf extract were prepared as nematocidal silver nanoparticles (AgNPs). The characterization and confirmation of the size of the Ag- NNPs were done using UV-Visible spectrophotometry and scanning electron microscopy (SEM) [7]. Also, the antimicrobial analysis was done for various microorganism to determine the bactericidal effect of the AgNPs. Results revealed that the green synthesized metal nematocidal nanoparticle might be the safe, potential and cost effective component which can be an alternatives to the chemical nematicide [8]. In the present study, the screened compounds were analysed *in-silico* against *Ralstonia solanacearum* through molecular docking approach. Following are the software used to carry out the molecular docking procedure and its analysis.

List of software used in this study to carry out in silico analysis:

(I). SWISS-MODEL

This is a fully automated protein homology modelling server that can be accessed by the Expasy web server. Amino acid sequence of the target protein is given as input in FASTA format which generates a 3D protein model by inducing experimental data from an evolutionary related protein structure that serves as a template. The quality of the assessed models is evaluated by QMEAN scoring function [9]. (<https://swissmodel.expasy.org/>)

(II). GalaxyRefine

This is one of the tools of the GalaxyWeb web server. A thorough protein structure relaxation is achieved by initial rebuilding of the 3D structure, repacking and finally by molecular dynamic simulations [10]. (<http://galaxy.seoklab.org/>)

(III). MolProbity 4.2

A web application that combines all atom contact analysis and is integrated with tools for validating covalent-geometry and torsion-angles of the macromolecular structure models. It also determines where residues fall in the multi-dimensional distributions of Ramachandran backbone  $\phi$ ,  $\psi$  angles and sidechain rotamer  $\chi$  angles [11]. (<http://molprobity.manchester.ac.uk/index.php>)

(IV). ACD/ChemSketch v2020.1.2

A free drawing package that enables chemical structures such as organics, organometallics, polymers, and structures of Markush to be drawn. It also includes features such as molecular property measurement (e.g., molecular weight, density, molar refractivity, etc.), cleaning and viewing of 2D and 3D structures, structure naming functionality, and logP prediction [12].

(V). ArgusLab

A free licensed molecular modelling and graphical tool used in this study for energy minimization and to clean up the geometry of the 3D structures prior to docking process [13].

(VI). CASTp 3.0

Computed Atlas of Surface Topography of proteins (CASTp) is an online tool for determining concave surface regions on protein structures. The output is given in the form of binding pockets located on protein surfaces and voids buried in the interior of proteins. This tool calculates the area and volume of the pockets covering the binding residues [14].

(VII). PyRx 0.8

A virtual screening software that includes vina and Autodock 4.2 docking wizard with a user-friendly interface which makes it a useful tool for Computer-Aided Drug Design. The key results obtained from the virtual screening runs are the best predicted binding poses and corresponding binding energy values. [15].

(VIII). UCSF Chimera 1.14

A molecular visualization program comprising a set of tools for interactive analyses of structures and sequences. This software offers 3D visualization of molecular structures in various presets along with supramolecular assemblies, density maps, multiple sequence alignments, energy minimization and molecular dynamics trajectories. For the purpose of publications and presentations, the user can also create images and animations using the tools provided by the software [16].

(IX). PyMOL 2.4

It is open-source, user-friendly and free visualization software package distributed by Schrödinger. This program can produce high-quality 3D images of intermolecular interactions of small molecules and biological macromolecules. Bond angles and distances can be measured easily. With scripting support, structures can be studied in a semi-automated way [17].

## MATERIAL AND METHODS

### Homology Modeling and Protein Preparation

The X-ray crystallographic structure of putative ketopantoate reductase from *Ralstonia solanacearum* MolK2 (PDB ID: 3GHY) with resolution 2.00 Å was retrieved from the Research Collaboratory for Structural Bioinformatics (RCSB) Protein Data Bank (PDB) (Fig.1). The protein sequence of putative cathepsin L protease of *Meloidogyne incognita* organism (GenBank: CAD89795.1) was taken from National Centre for Biotechnology Information (NCBI) This sequence was considered to generate a homology- modelled structure as the 3D structure was unavailable in the structural databases [18]. The three-dimensional coordinates for the protein sequence were generated using SWISS-MODEL, accessible by the Expasy web server (Fig.2).

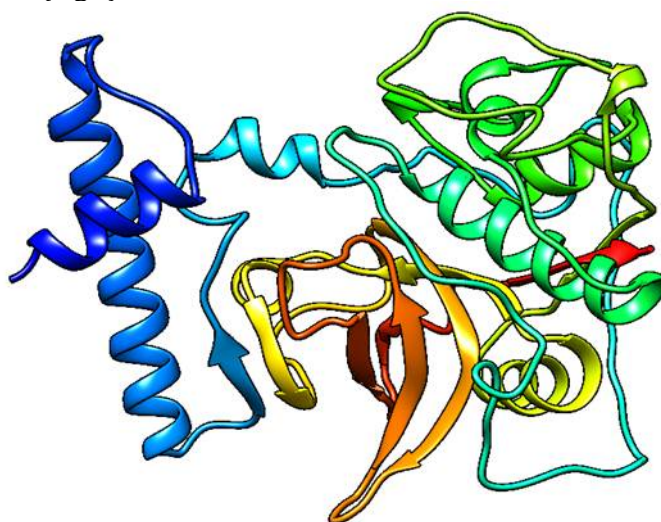


**Fig.1.** Three-dimensional structure of putative ketopantoate reductase from *Ralstonia solanacearum* MolK2 having single chain A

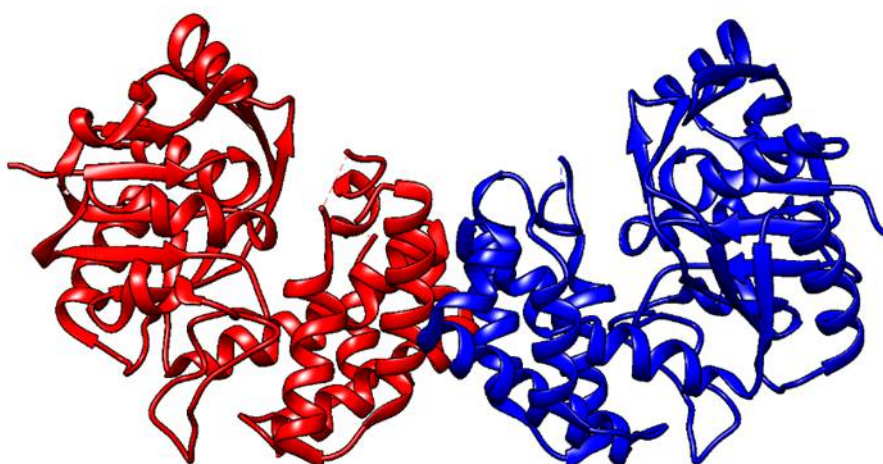


**Fig. 2.** The ribbon structure of SWISS-MODEL homology modelled protein of putative cathepsin L protease of the root-knot nematode *Meloidogyne incognita*

### Protein Refinement and Validation

The protein targets were refined using a refinement tool, GalaxyRefine of GalaxyWeb web server [19]. It is also possible to refine 3D models by changing secondary structure units and repacking sidechains and get them closer to native structures [20]. The quality of both the 3D protein structures were validated and quality of the models were then evaluated using validation software, MolProbity.

### Ligand Preparation

Among all identified phytochemicals of *Alstonia macrophylla* [21] and *Argemone Mexicana* [22], three anti-bacterial phytochemicals complexed with silver nanoparticles, Caffeic acid AgNPs, Dioctyl phthalate AgNPs and ProlylglycineAgNPs were preferred for *in silico* molecular docking analysis with bacterial and nematode molecular targets [23]. The structures of these ligands were drawn using ACD-Chemsketch and saved as MOL file and further converted to PDB using Open Babel GUI tool by generating 3D coordinates and adding the hydrogen atoms. The structure of the standard drug, streptomycin taken for the reference was obtained from NCBI PubChem compound database (Fig.3) [24]. Energy minimization for all the ligands was done to remove clashes among atoms of the ligand and the structures were cleaned prior to docking in ArgusLab to obtain stable conformations [25].

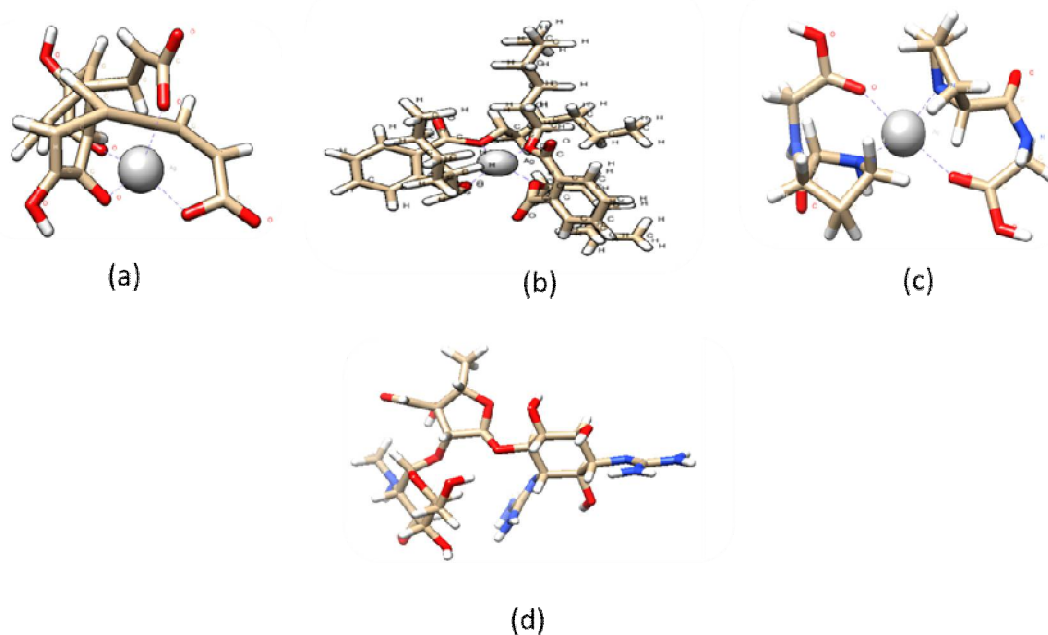


**Fig.3.** Three-dimensional structures of ligand complexes (a) Caffeic acid AgNPs (b) Dioctyl phthalate AgNPs (c) ProlylglycineAgNPs sketched using ChemSketch software and structure of standard drug (d) streptomycin retrieved from PubChem.

### Binding Site Identification

Protein ligand binding pocket on the target proteins were identified using the CASTp server which gives multiple active sites as output along with the values of area and volume covered by each pocket [26] The binding pocket was then determined by choosing the specific residues in PyRx prior to docking run. The grid box was adjusted accordingly surrounding the highlighted binding residues of the protein structures [27].

### Molecular Docking

Prior to docking both the target structures were prepared by stabilizing charges, filling the missing residues followed by removing crystallographic water molecules. This makes the target proteins stable and biologically active [28]. The grid-based molecular docking was carried out using PyRx software and only the finest scoring fit with binding score was noted for each small molecule [29]. The binding residues of the target proteins were held rigid while the ligands are allowed to be flexible which gives 10 poses of each ligand. The docking scores were recorded, and docking poses were saved for reference [30]. Out of the 10 docked poses, the binding pose having the least binding energy (Kcal/mol) of each ligand were considered to analyse further for non-covalent interactions using UCSF Chimera and PyMOL visualization software [31].

## RESULTS

### Protein Validation

The structures refined to improve the quality of bond angles, bond lengths and change in rotamers. The refined structure exhibited a change in the N-terminal structure, particularly concerning the defined helices.

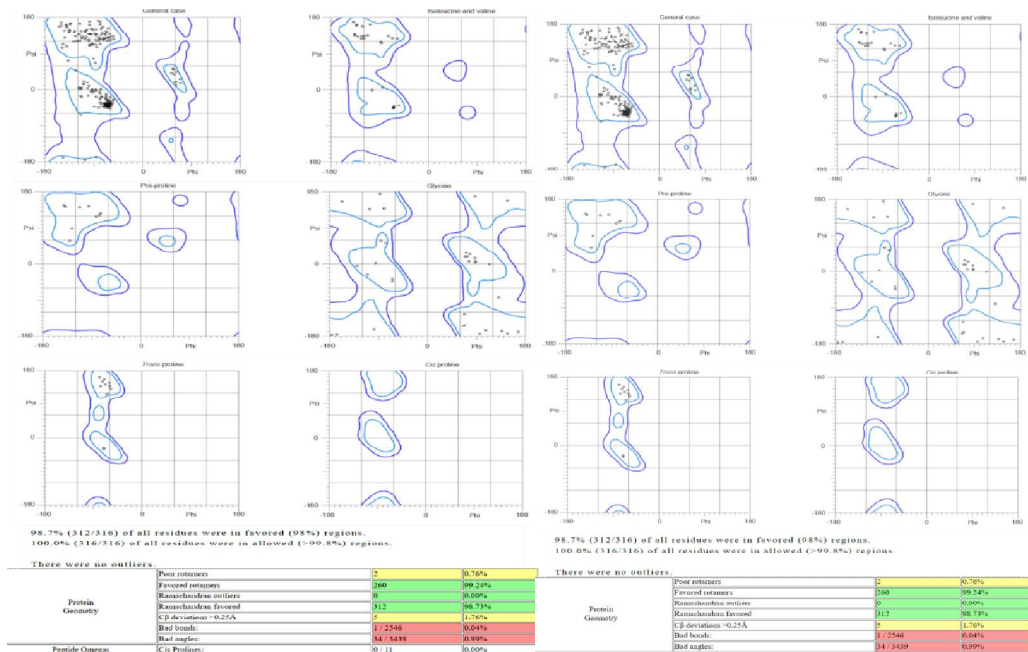
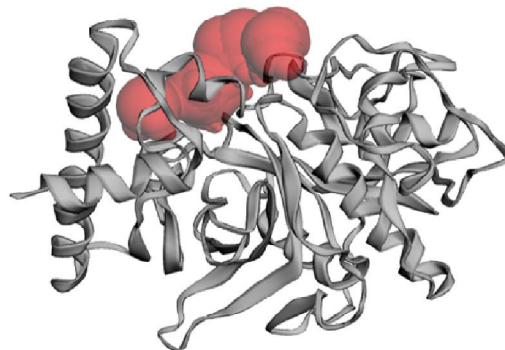


**Fig.4. Structure validation report of the modelled protein of putative ketopantoate reductase and PDB protein-3 GHY post refinement showing 98.7% and 94.8% residues in favoured region.**

**Prediction of Binding Site**

Using the CASTp server ,a single binding pocket was generated for both the proteins [32].The area covered by the binding pocket of the homology-modeled structure of putative cathepsinL protease was sought to be 311.508 and the volume was 270.506 while that of the PDBprotein,3GHY was 1103.278 and 739.190 respectively. In Fig. 5 and 6, the active pocket is appeared in red color surrounding the highlighted binding residues in the sequence.



Sequence

Chain A

R G F A D W Q A Y K E K H G K S Y P H Q D E D N E R H L A Y L S A K Q F I E K H Q R D Y T E G R V S F Q V G E N H H A D V P F N Q Y R K L N G

F X R L L G D A V T R K N A S S T F L P P L N H Y A I P E S V D H R D K G L V T S V K N Q G M C G S C H A F S A T G A L E G Q H S R K L G T L

V S L S E Q N L I D C T K G E P Y G N H G C N G G L R D N A F Q Y I E D N K G V D T E N S Y P Y K A N G K K C L F K R S N V G A T D T G Y V

D L P S G D E D K L I A V A T Q G P I S V A I D A G H R S F Q L V A H G V Y D E E A C S P D H L G H G V L V V G Y G T D D I H G D Y H L V K

N S M G E H M G E N G Y I R M S R N K D N Q C G I A S K A S Y P L V

**Fig. 5. The surface of the binding pocket (red coloured) of the modelled protein along with its sequence which highlights the binding residues as computed using CASTp.**

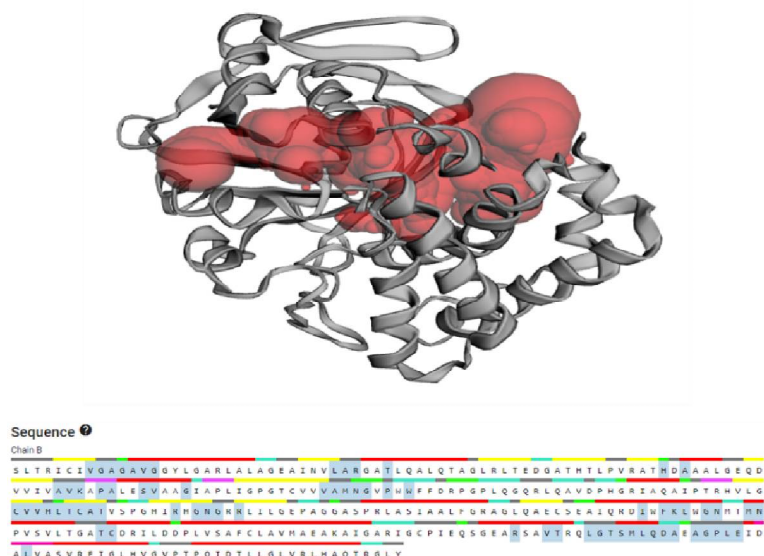


**Fig. 6.** The binding residues of the PDB protein, 3GHY enclosed by the active binding pocket appeared in red colour as predicted by CASTp.

### Molecular Docking Analysis

The docking results confirmed that all the phytochemicals obtained from the extract interacted well with the protein targets in comparison with the standard drug. The best docked pose out of 10 docked poses of each protein-ligand docking having the least binding energy was chosen [33]. The docked poses of the ligands with the target proteins provide a good image of the ligand-target protein binding. The number of hydrogen bonds and other non-covalent interactions determine the docking's stability. **Table 1** shows the total number of hydrogen bonds and the unique residues involved in each ligand's hydrogen bonding with its respective protein. In this study, putative cathepsin L protease of the root-knot nematode *M. incognita* and putative ketopantoate reductase from *Ralstonia solanacearum* were docked with three phytochemicals complexed with silver nanoparticles.

**Table 1:** Ligand-receptor interactions and binding energy value of the best docked pose of each ligand with highest binding affinity.

Sl. No.	Protein	Ligands	Binding Energy (Kcal/mol)	Number of Hydrogen bonds	Hydrogen bond forming amino acids
1	Putative cathepsin L protease [ <i>Meloidogyne incognita</i> ]	Caffeic acid AgNPs	-7.7	3	Lys-138, asp-303, leu-327
		Diethyl phthalate AgNPs	-5.6	2	Asn-135, lys-138
		ProlylglycineAgNPs	-7.7	9	Asn-135, lys-138, asn-230, ala-304, asn 326, leu-327
		Streptomycin	-6.6	4	Arg-132, asn-135, lys-138
2	Putative ketopantoate reductase from <i>Ralstonia solanacearum</i> MolK2 (PDB ID: 3GHY)	Caffeic acid AgNPs	-8.9	7	Ala-11, val-12, ala-75, asn-103, glu-286
		Diethyl phthalate AgNPs	-4.5	1	Asp-288
		ProlylglycineAgNPs	-7.9	7	Val-76, asn-103, thr-147, cys-148, lys-204, ser-273, glu-286
		Streptomycin	-8.0	3	Val-12, lys-77, ser-273

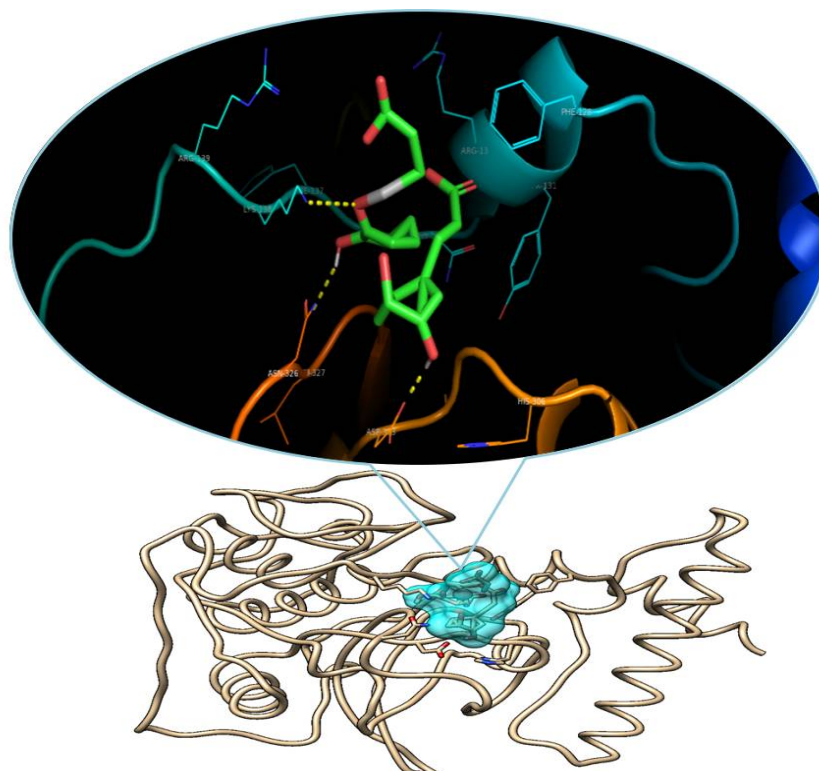


**Fig. 7.** Binding mode of Caffeic acid silver nanoparticles complex with active site of putative cathepsin L protease of *Meloidogyne incognita* modelled protein. Three intermolecular, yellow coloured hydrogen bonds can be visualized.

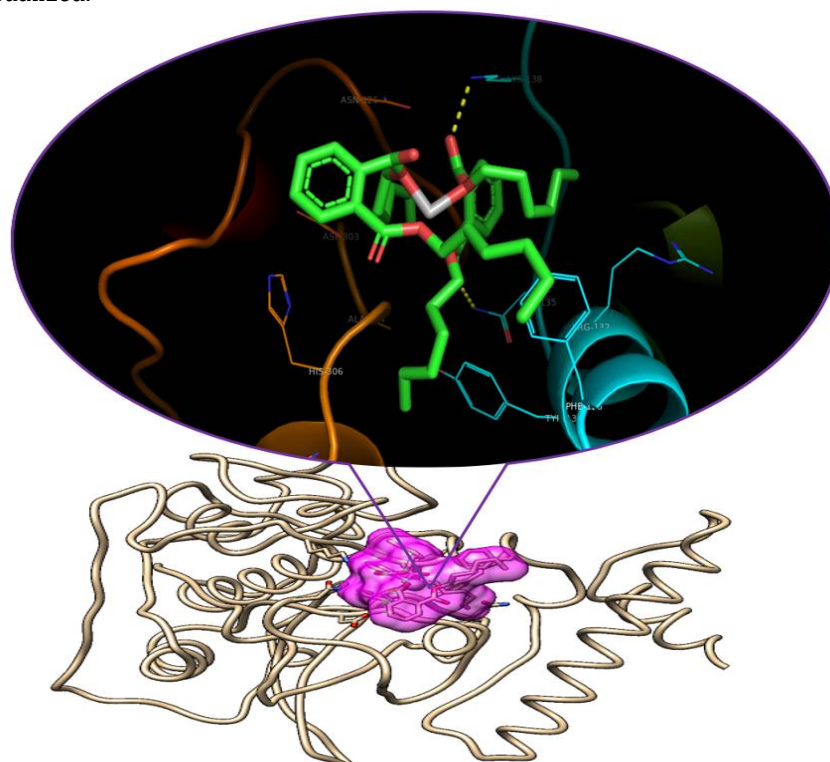


**Fig.8.** Binding mode of Dioctyl phthalate silver nanoparticles complex with active site of putative cathepsin L protease of *Meloidogyne incognita* modelled protein. Two intermolecular, yellow coloured hydrogen bonds can be visualized.

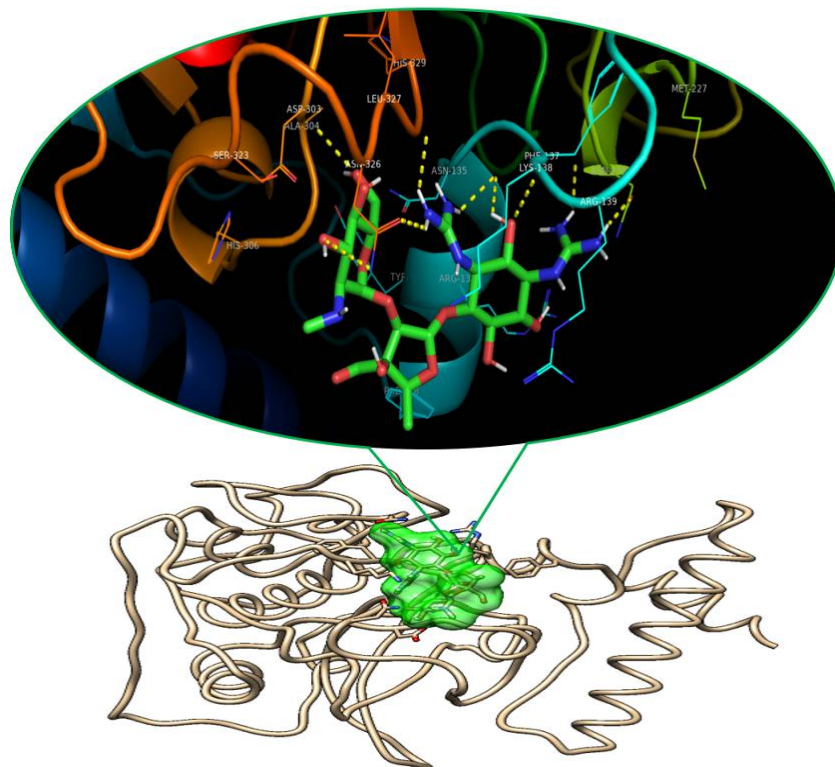


**Fig.9:** Binding mode of Prolylglycine silver nanoparticles complex with active site of putative cathepsin L protease of *Meloidogyne incognita* modelled protein. Nine intermolecular, yellow coloured hydrogen bonds can be visualized.

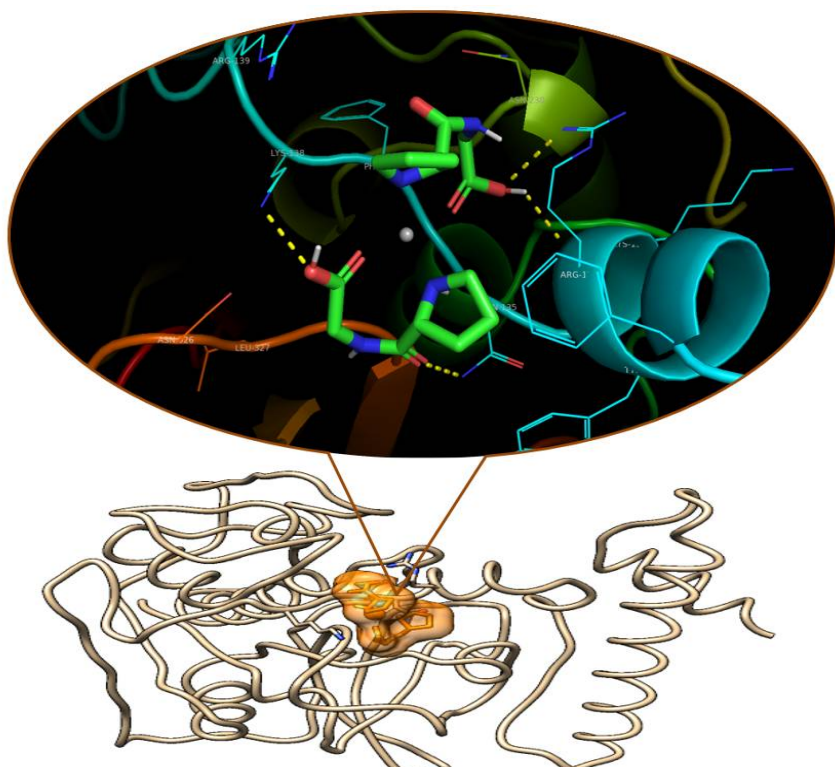


**Fig.10:** Pictorial 3D representation of the standard drug, streptomycin bound to the active pocket of putative cathepsin L protease of *Meloidogyne incognita* modelled protein via four hydrogen bonds.

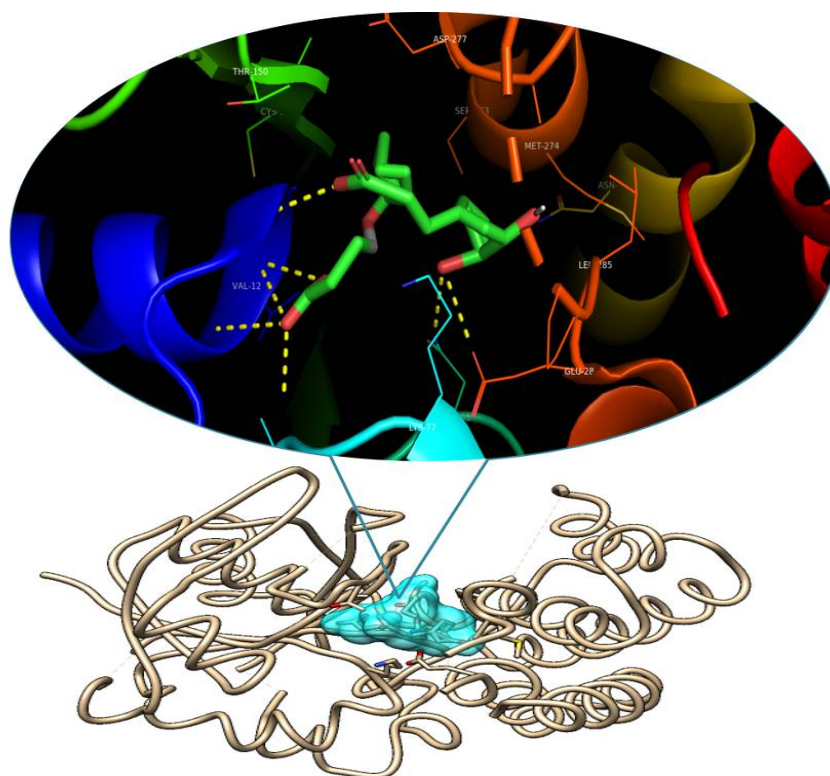


**Fig.11:** Binding mode of Caffeic acid silver nanoparticles complex with active site of putative ketopantoate reductase from *Ralstonia solanacearum* MolK2 (PDB ID:3GHY). Seven intermolecular, yellow coloured hydrogen bonds can be visualized.

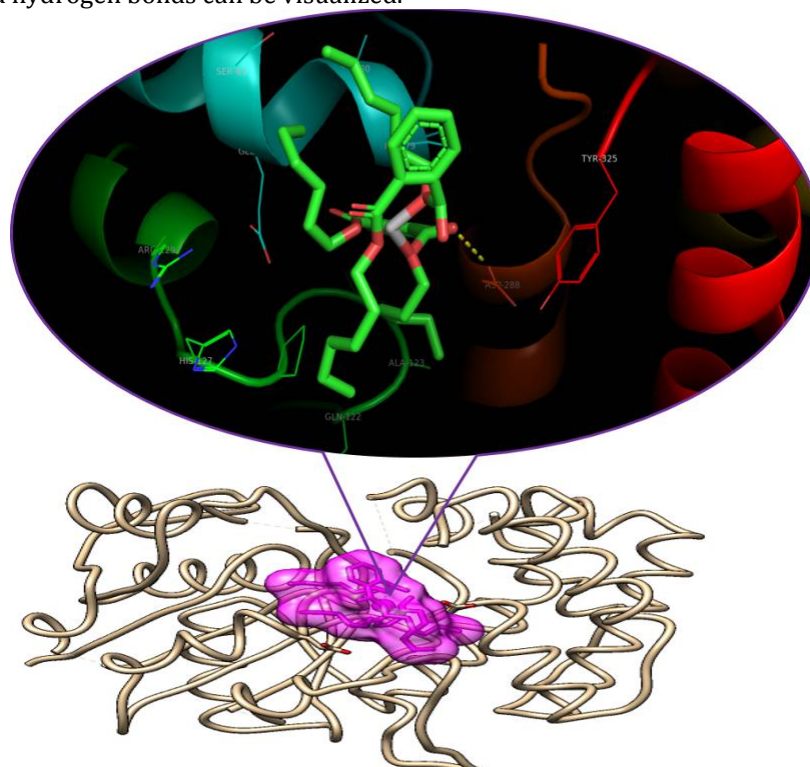


**Fig.12:** Binding mode of Dioctyl phthalate silver nanoparticles complex with active site of putative ketopantoate reductase from *Ralstonia solanacearum* MolK2 (PDB ID:3GHY). Only a single intermolecular, yellow coloured hydrogen bond can be visualized.

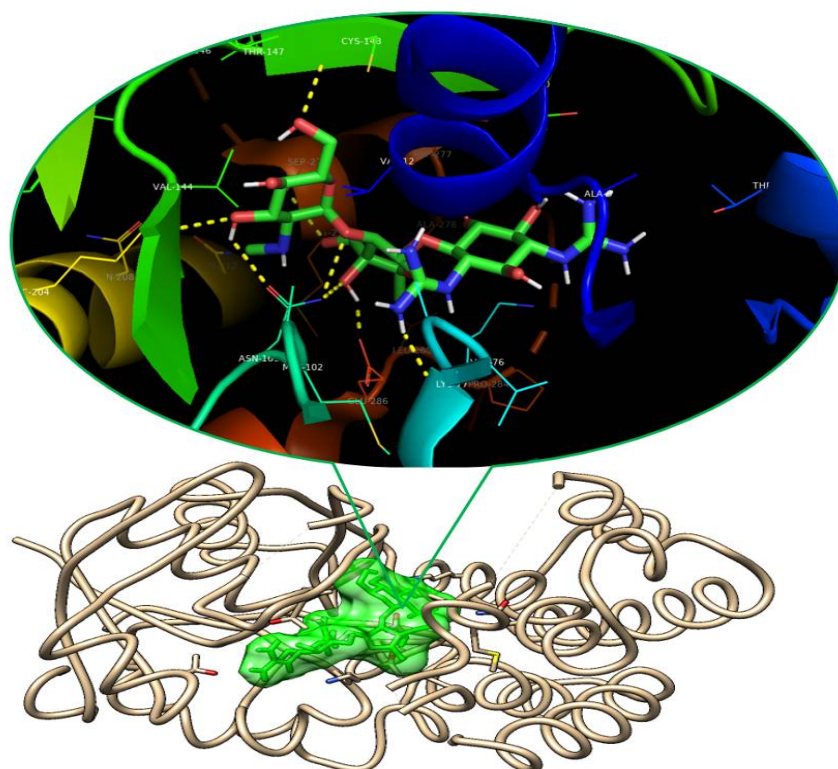


**Fig.13:** Binding mode of Prolylglycine silver nanoparticles complex with active site of putative ketopantoate reductase from *Ralstonia solanacearum* MolK2 (PDB ID:3GHY). Seven intermolecular, yellow coloured hydrogen bonds can be visualized.

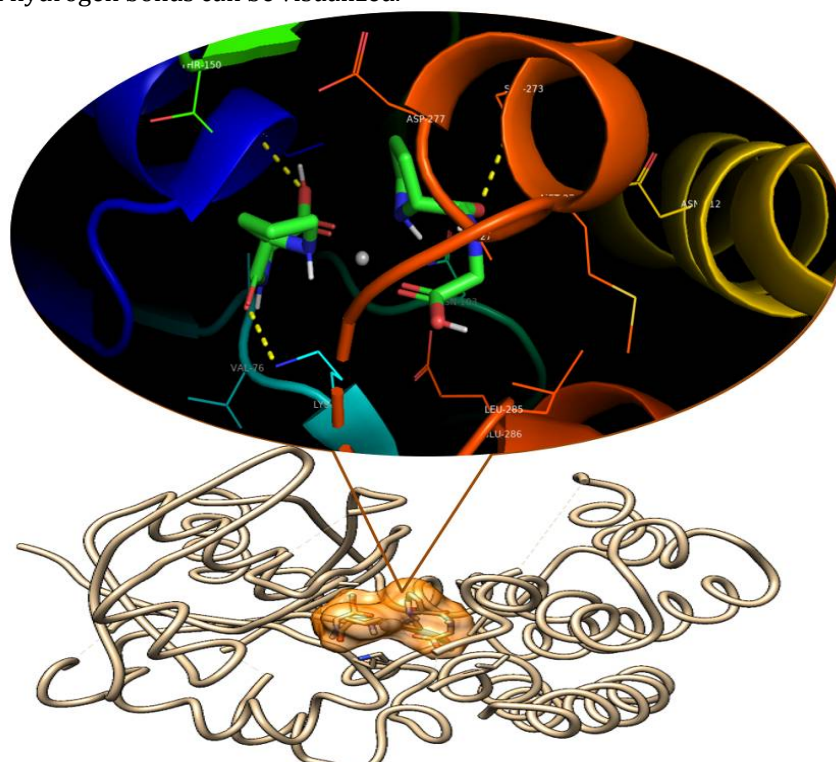


**Fig.14:** Pictorial 3D representation of the standard drug, streptomycin bound to the active pocket of putative ketopantoate reductase from *Ralstonia solanacearum* (PDB ID:3GHY) via four hydrogen bonds.

## DISCUSSION

A key feature of the three-dimensional structure of proteins is that they can bind to other small molecules or proteins with high affinity and specificity. This binding is determined by the shape of the binding active

pocket along with the physiochemical properties of the amino acid residues forming the pocket [34]. Molecular docking is a tool to find the most favorable binding pose of a receptor molecule relative to another when a complex is formed [35]. A blend of intermolecular interactions which include van der Waals, electrostatic, hydrophobic interactions and hydrogen bonds describes the protein- ligand interactions [36]. The structure of a protein-ligand complex at the atomic level is essential for molecular docking studies.

The intermolecular interactions were observed using UCSF Chimera and PyMOL for evaluating the results. The ligand is expected to bind to a target protein if the binding affinity (or binding free energy) is negative [37]. The stronger the expected interaction between a ligand and a macromolecule, the lower the binding affinity values are [38]. The highest binding affinity compounds results for the docked compounds having the least binding energy value.

## CONCLUSION

The screened compounds complexed with AgNPs were interacted *in-silico* against the selected proteins of *Ralstonia solanacearum*. Observing the molecular docking and molecular interaction, binding energy, and distance between the target 3GHY, modelled protein and selected ligands, it is found that the ligands are capable to exhibit the modulatory functions. Further, these nanoparticles were tested for their in-vitro antimicrobial activity and the results revealed that these nanoparticles inhibited the growth of *Ralstonia solanacearum*.

## REFERENCES

1. Satterthwaite, D., McGranahan, G. & Tacoli C. (2010). Urbanization and its implications for food and farming. *Phil. Trans. R. Soc. B.*, 365:2809–2820.
2. Bashyal, B.M., Rawat, K., Sharma, S., Gogoi, R. & Aggarwal, R. (2020). Major Seed-Borne Diseases in Important Cereals: Symptomatology, Aetiology and Economic Importance. In *Seed-Borne Diseases of Agricultural Crops: Detection, Diagnosis & Management*. Springer, Singapore. pp. 371-426
3. Shin, J., Prabhakaran, V.S. & Kim, K.S. (2018). The multi-faceted potential of plant-derived metabolites as antimicrobial agents against multidrug-resistant pathogens. *MicrobPathog.*, 116:209-14.
4. Peralta, I.E. & Spooner, D.M. (2006). History, origin and early cultivation of tomato (Solanaceae). *Genetic improvement of solanaceous crops*, Vol. 2. Enfield, USA: Science Publishers. pp. 1-27
5. Gajc-Wolska, J., Korzeniewska, A. J. Benton Jones Jr. (2009) Tomato plant. Culture in the field, greenhouse, and home garden. *Acta Physiol Plant* 31, 425–426.
6. El-Deen A.N. & El-Deeb, B.A. (2008). Effectiveness of silver nanoparticles against root-knot nematode, *Meloidogyne incognita* infecting tomato under greenhouse conditions. *J Agric Sci.*, 10(2):148-56.
7. Thurlow, C. (1995). The Amazingly Simple Banana Diet. Maximilian Thurlow. pp 96.
8. Waterhouse, A., Bertoni, M., Bienert, S., Studer, G., Tauriello, G., Gumienny, R., Heer, F.T., de Beer, T.A.P., Rempfer, C., Bordoli, L., Lepore, R. & Schwede, T. (2018) SWISS-MODEL: homology modelling of protein structures and complexes. *Nucleic Acids Res.*, 46(W1): W296-W303.
9. J. Ko., H. Park., L. Heo., & C. Seok. (2012). GalaxyWEB server for protein structure prediction and refinement. *Nucleic Acids Res.*, 40(W1):W294-W297.
10. Chen, V. B., Arendall, W. B., 3rd, Headd, J. J., Keedy, D. A., Immormino, R. M., Kapral, G. J., Murray, L. W., Richardson, J. S., & Richardson, D. C. (2010). MolProbity: all-atom structure validation for macromolecular crystallography. *Acta Crystallogr D Biol Crystallogr.*, 66(Pt 1):12-21.
11. ACD/ChemSketch, version 2020.1.2, Advanced Chemistry Development, Inc., Toronto, ON, Canada, www.acdlabs.com.
12. Thompson, M.A. (2004) Molecular Docking Using ArgusLab, an Efficient Shape-Based Search Algorithm and the Score Scoring Function. ACS Meeting, Philadelphia.
13. Wei, Tian., Chang, Chen., Xue, Lei., Jieling, Zhao. & Jie, Liang. (2018). CASTp 3.0: computed atlas of surface topography of proteins. *Nucleic Acids Res.*, 46(W1), W363–W367.
14. Dallakyan, S. & Olson, A.J. (2015). Small-molecule library screening by docking with PyRx. *Methods Mol Biol.*, 1263:243-50.
15. Sanner, M.F., Olson, A.J. & Spehner, J.C. (1996). Reduced surface: an efficient way to compute molecular surfaces. *Biopolymers.*, 38(3):305-320.
16. The PyMOL Molecular Graphics System, Version 2.0 Schrödinger, LLC.
17. Berman, H. M., Westbrook, J., Feng, Z., Gilliland, G., Bhat, T. N., Weissig, H., Shindyalov, I. N., & Bourne, P. E. (2000). The Protein Data Bank. *Nucleic acids res.*, 28(1), 235–242.
18. Neveu, C., Jaubert, S., Abad, P., & Castagnone-Sereno, P. (2003). A set of genes differentially expressed between avirulent and virulent *Meloidogyne incognita* near-isogenic lines encode secreted proteins. *Mol Plant Microbe Interact.*, 16(12):1077-84.
19. Shruthi, G., Joyappa, M.P., Chandrashekhar, S., Kollur, S.P., Prasad, M.N., Prasad, A., Shivamallu, C. (2017). Bactericidal property of *Clerodendrum paniculatum* and *Saraca asoka* against multidrug resistant bacteria, restoring the faith in herbal medicine. *Int J Pharm Sci Res.*, 8(9), 3863-71.
20. McDade, J.J., Weaver, R.H. (1959). Rapid methods for the detection of gelatin hydrolysis. *Journal of bacteriology.*,

- 77(1),60.
21. Wood, J.M. (1967). The amount, distribution and metabolism of soluble polysaccharides in human dental plaque. *Archives of oral biology*,12(7),849-58.
  22. Walters,G.R.,Plumb,J.A.(1978).Modified oxidation/fermentation medium for use in identification of bacterial fish pathogens.*Journal of the Fisheries Board of Canada*, 35(12),1629-30.
  23. Goñi, I, Garcia-Alonso, A, Saura-Calixto, F. (1997). A starch hydrolysis procedure to estimate glycemic index. *Nutrition Research*,17(3),427-37.
  24. Kovac,S,Angelova,P.R.,Holmström,K.M.,Zhang,Y.,Dinkova-Kostova,A.T.,AbramovAY. (2015).Nrf2 regulates ROS production by mitochondria and NADPH oxidase. *Biochimicaet Biophysica Acta(BBA)-General Subjects*,1850(4),794-801.
  25. Wang, H, Qi, M., Cutler, A.J. (1993). A simple method of preparing plant samples for PCR.*Nucleic acids research*,21(17);4153.
  26. Müller, L, Fröhlich, K, Böhm, V. (2011). Comparative antioxidant activities of carotenoids measured by ferric reducing antioxidant power (FRAP), ABTS bleaching assay( $\alpha$ TEAC), DPPH assay and peroxy radical scavenging assay. *Food Chemistry*,129(1),139-48.
  27. Sroka, Z, Cisowski, W. (2003). Hydrogen peroxide scavenging, antioxidant and anti-radical activity of some phenolic acids. *Food and Chemical Toxicology*,41(6),753-8.
  28. Zacheo, G, Bleve-Zacheo, T, Lamberti, F. (1982). Role of peroxidase and superoxidisedismutase activity in resistant and susceptible tomato cultivars infested by *Meloidogyne incognita*. *Nematologia mediterranea*.234-246
  29. Adiyaman, R. & McGuffin, L.J. (2019). Methods for the Refinement of Protein Structure 3D Models. *Int J Mol Sci*, 20(9):2301.
  30. Chattopadhyay, D, Maiti, K, Kundu, A.P., Chakraborty, M.S, Bhadra, R, Mandal, S.C. & Mandal, A.B. (2019). Antimicrobial activity of *Alstonia macrophylla*: a folklore of bay islands. *J Ethnopharmacol*,77(1):49-55.
  31. Jain, A. S, Sushma, P, Dharmashekar, C, Beelagi, M. S, Prasad, S. K, Shivamallu, C, Prasad, A, Syed, A, Marraiki, N, & Prasad, K. S. (2021). In silico evaluation of flavonoids as effective antiviral agents on the spike glycoprotein of SARS-CoV-2. *Saudi J Biol Sci*,28(1), 1040-1051.
  32. El-Naggar, M, Mohamed, M. E., Mosallam, A. M., Salem, W., Rashdan, H. R., & Abdelmonsef, A. H. (2020). Synthesis, Characterization, Antibacterial Activity, and Computer-Aided Design of Novel Quinazolin-2,4-dione Derivatives as Potential Inhibitors Against *Vibrio cholerae*. *EvolBioinform Online*, 16, 1176934319897596.
  33. Butt, S, Badshah, Y, Shabbir, M. & Rafiq, M. (2020). Molecular Docking Using Chimera and Autodock Vina Software for Non-bioinformaticians. *JMIR Bioinformatics Biotechnol*, 1(1):e14232.
  34. Avinash, K.O, Sushma, P, Chandan, S, Gopenath, T.S, Kiran, M.N, Kanthesh, B.M, Kumar, J.R. (2021). In Silico Screened Flavanoids of *Glycyrrhiza glabra* Inhibit Cpla2 And Spla2 In Lps Stimulated Macrophages. *Bull. Env. Pharmacol. Life Sci*,10(4): 14-24.
  35. Prasad, A, Govindaraju, S, Sushma, P, et al. (2020). *Helicobacter pylori* infection : a bioinformatic approach. *International Journal of Pharmaceutical Sciences and Research*, 11, 5469-83.
  36. Ankegowda, V.M, Kollur, S.P, Prasad, S.K, Sushma, P, Dhramashekar, C, et al. (2020). Phyto-Mediated Synthesis of Silver Nanoparticles Using *Terminalia chebula* Fruit Extract and Evaluation of Its Cytotoxic and Antimicrobial Potential. *Molecules*, 25, 5042.
  37. Prasad, S.K, Pradeep, S, Shimavallu, C, Kollur, S.P, Syed, A, Marraiki, N, Egbuna, C, Gaman, M-A, Kosakowska, O, Cho, W.C, Patrick-Iwuanyanwu, K.C, Ortega, C.J, Frau, J, Flores-Holguín, N and Glossman-Mitnik, D. (2021). Evaluation of *Annona muricata* Acetogenins as Potential Anti-SARS-CoV-2 Agents Through Computational Approaches. *Front. Chem*, 8,624716.
  38. Kollur, S.P, Prasad, S.K, Pradeep, S, Veerapur, R, Patil, S.S, Amachawadi, R.G, Lamraoui, G, Al-Kheraif, A.A, Elgorban, A.M, Syed, A, Shivamallu, C. (2021). Luteolin-Fabricated ZnO Nanostructures Showed PLK-1 Mediated Anti-Breast Cancer Activity. *Biomolecules*, 11(3),385.

#### CITATION OF THIS ARTICLE

Navyashree B, Anisha S Jain, Sushma P, Chandan D, Sharagouda S Patil, Shiva Prasad Kollur, Latha KC and Chandan S. A Computational based approach in discovering the phytocompound based complex inhibition against *Ralstonia solanacearum* and root-knot nematode *Meloidogyne incognita*. *Bull. Env. Pharmacol. Life Sci*, Vol 10[11] October 2021 :30-41.